J Physiol 587.17 (2009) pp 4235–4247

The Journal of Physiology

Excitability of paraventricular nucleus neurones that project to the rostral ventrolateral medulla is regulated by small-conductance Ca^{2+}-activated K^+ channels

Qing-Hui Chen and Glenn M. Toney

Department of Physiology, University of Texas Health Science Center at San Antonio, San Antonio, TX 78229-3900, USA

Whole cell patch-clamp recordings were performed in brain slices to investigate mechanisms regulating the excitability of paraventricular nucleus (PVN) neurones that project directly to the rostral ventrolateral medulla (RVLM) (PVN–RVLM neurones) of rats. In voltage-clamp recordings, step depolarization elicited a calcium-dependent outward tail current that reversed near E_K. The current was nearly abolished by apamin and by UCL1684, suggesting mediation by small-conductance Ca^{2+}-activated K^+ (SK) channels. In current-clamp recordings, depolarizing step current injections evoked action potentials that underwent spike-frequency adaptation (SFA). SK channel blockade with apamin or UCL1684 increased the spike frequency without changing the rate of SFA. Upon termination of step current injection, a prominent medium after-hyperpolarization potential (mAHP) was observed. SK channel blockade abolished the mAHP and revealed an after-depolarization potential (ADP). In response to ramp current injections, the rate of sub-threshold depolarization was increased during SK channel blockade, indicating that depolarizing input resistance was increased. Miniature EPSC frequency, amplitude, and decay kinetics were unaltered by bath application of apamin, suggesting that SK channel blockade likely increased excitability by a postsynaptic action. We conclude that although SK channels play little role in generating SFA in PVN–RVLM neurones, their activation nevertheless does dampen excitability. The mechanism appears to involve activation of a mAHP that opposes a prominent ADP that would otherwise facilitate firing.

(Received 12 May 2009; accepted after revision 6 July 2009; first published online 6 July 2009)

Corresponding author Q.-H. Chen: Department of Physiology–MC7756, University of Texas Health Science Center, 7703 Floyd Curl Drive, San Antonio, TX 78229-3900, USA. Email: chenq@uthscsa.edu

Abbreviations ADP, after-depolarization potential; AHP, after-hyperpolarization potential; 8CPT-cAMP, cAMP analogue 8-(4-chlorophenylthio) 3′,5′-cyclic adenosine monophosphate; ISI, inter-spike interval; mEPSC, miniature excitatory postsynaptic current; PVN, paraventricular nucleus; RVLM, rostral ventrolateral medulla; SFA, spike-frequency adaptation; SK, small-conductance Ca^{2+}-activated K^+; SNA, sympathetic nerve activity.

A widely distributed CNS network generates and regulates rhythmic activity in peripheral sympathetic nerve activity (SNA) that is essential for maintaining arterial blood pressure and cardiovascular homeostasis (Guyenet, 2006). Among neurones comprising this network, presympathetic neurones in the hypothalamic paraventricular nucleus (PVN) have been the focus of considerable interest now for many years (Porter & Brody, 1985; Lovick & Coote, 1988; Stern 2001; Allen 2002; Akine *et al.* 2003; Toney *et al.* 2003; Li & Pan, 2007). The picture that has emerged indicates that discharge of these neurones is normally suppressed by strong GABA-mediated synaptic inhibition (Martin *et al.* 1991; Chen *et al.* 2003; Li *et al.* 2006). Consistent with this, electrophysiological studies demonstrate that most presympathetic PVN neurones are either quiescent or exhibit slow (1–2 spikes s^{-1}) irregular discharge *in vivo* (Lovick & Coote, 1988; Chen & Toney, 2000, 2003). Interestingly, interruption of PVN GABAergic inhibition increases SNA and transforms SNA burst discharge into a low frequency, high amplitude pattern (Kenney *et al.* 2001). The latter suggests that ongoing synaptic inhibition may prevent burst firing of presympathetic PVN neurones.

In spite of having little tonic activity under normal conditions (Lovick & Coote, 1988; Chen & Toney, 2000, 2003) and contributing only modestly to the maintenance of ongoing SNA (Allen, 2002), presympathetic PVN neurones are nevertheless considered essential for increasing SNA under a variety of circumstances; including during physiological perturbations (e.g.

DOI: 10.1113/jphysiol.2009.175364

dehydration, hypoxaemia, etc.) (Stocker *et al*. 2005; Reddy *et al*. 2007; Cruz *et al*. 2008) and during more chronic disease conditions (e.g. heart failure, hypertension, cardiac ischaemia, etc.) (Haywood *et al*. 2001; Li & Pan, 2006; Patel, 2008). Haywood and colleagues, for example, reported that GABAergic inhibition of the PVN is reduced in rats with renal-wrap hypertension in which elevated blood pressure is maintained, at least in part, by elevated SNA (Haywood *et al*. 2001). Using the same hypertensive model, the Stern laboratory recently reported that the intrinsic excitability of presympathetic PVN neurones is increased in association with a reduction of the transient A-type potassium current (Sonner *et al*. 2008). Thus, persistently elevated discharge of PVN neurones appears to be achieved both by changing their synaptic input (i.e. decreased inhibition and/or increased excitation) and by modifying their intrinsic membrane properties.

Evidence indicating that PVN neurones are important for setting the level of SNA prompted interest in mechanisms that regulate their excitability and discharge. Many studies have focused on PVN neurones that project directly to the rostral ventrolateral medulla (RVLM), as the latter region is the major source of excitatory synaptic drive to spinal sympathetic preganglionic neurones. PVN–RVLM neurones make close synaptic appositions with sympathoexcitatory RVLM neurones and are mostly glutamatergic (Stocker *et al*. 2006), though they may co-express a number of neuropeptides. In keeping with this, studies performed in intact rats indicate that PVN stimulation increases the discharge of bulbospinal RVLM neurones by activating ionotropic glutamate receptors and vasopressin V_1 receptors (Yang & Coote, 1998; Yang *et al*. 2001).

In brain slice studies, presympathetic PVN neurones exhibit complex patterns of discharge. Application of L-glutamate, for example, evokes high frequency trains of action potentials followed by significant postexcitatory depression (Pakhomov *et al*. 2006). A similar pattern of discharge has been observed among PVN–RVLM neurones in response to the neuropeptide angiotensin II (Cato & Toney, 2003) and in response to depolarizing current injections, which also elicit high frequency discharge accompanied by significant spike-frequency adaptation (SFA) and a prominent after-hyperpolarization potential (AHP) (Tasker & Dudek, 1991; Stern, 2001; Sonner & Stern, 2007). Based on literature evidence that these activity patterns often result from activation of one or more Ca^{2+}-sensitive K^+ conductances subsequent to an increase in intracellular calcium (i.e. through activation of voltage-dependent Ca^{2+} channels) (Vogalis *et al*. 2003; Stocker, 2004; Villalobos *et al*. 2004; Teruyama & Armstrong, 2007, but see Teagarden *et al*. 2008), we hypothesized that small-conductance Ca^{2+}-activated K^+ (SK) channels suppress excitability of PVN–RVLM neurones and contribute to the patterning of their discharge. To test this hypothesis, the present study was conducted *in vitro* using hypothalamic slices. Whole cell patch-clamp recordings were performed in PVN–RVLM neurones identified by retrograde axonal tracing.

Methods

Animals

Male Sprague–Dawley rats ($n = 25$, 400–500 g) were purchased from Charles River Laboratories (Wilmington, MA, USA) and were individually housed in a temperature controlled room (22–23°C) with a 14 h–10 h light–dark cycle. Rats had free access to standard chow and tap water. All experimental and surgical procedures were approved by the Institutional Animal Care and Use Committee of the University of Texas Health Science Center at San Antonio and were performed in strict adherence to procedures set for the NIH *Guide to the Care and Use of Laboratory Animals*.

Retrograde labelling of PVN–RVLM neurones

PVN neurones were retrogradely labelled from the ipsilateral RVLM as previously described (Cato & Toney, 2005). Briefly, rats were anaesthetized with isoflurane (3% in O_2) and placed in a stereotaxic frame, and a small burr hole was made to expose the cerebellum. A glass micropipette was lowered into the pressor region of RVLM (co-ordinates: −12.7 mm caudal to bregma, 1.8 mm lateral to midline and 8.9 mm below the skull) and rhodamine-containing microspheres were microinjected in a volume of 50 nl. Each animal received a daily injection of penicillin G (30 000 units (100 g bw)$^{-1}$, S.C.) for 3 days after surgery. The location of the tracer was verified histologically (Cato & Toney, 2005; Stocker *et al*. 2006).

Electrophysiology

Five to seven days after tracer injections into RVLM, rats were anaesthetized with isoflurane (3% in O_2) and decapitated. Brains were removed and placed in ice-cold cutting solution containing (in mM): sucrose, 206; KCl, 2; $MgSO_4$, 2; NaH_2PO_4, 1.25; $NaHCO_3$, 26; $CaCl_2$, 1; $MgCl_2$, 1; D-glucose, 10; ascorbic acid, 0.4. Osmolarity and pH were adjusted to 290–295 mosmol l^{-1} and 7.4, respectively. Solution pH and P_{O_2} were maintained by equilibration with a 95% O_2–5% CO_2 gas mixture. Coronal slices through the PVN were cut to a thickness of 300 μm on a vibrating microtome (Leica VT 1000S; Leica, Nussloch, Germany). Slices were incubated at room temperature (24–26°C) for at least 2 h in continuously gassed artificial cerebrospinal fluid (ACSF) containing (in mM): NaCl, 125; KCl, 2; $MgSO_4$, 2; NaH_2PO_4, 1.25;

$NaHCO_3$, 26; $CaCl_2$, 2; D-glucose, 10; ascorbic acid, 0.4 (osmolarity 295–300 mosmol l^{-1}; pH 7.4). Slices were transferred to a glass-bottomed recording chamber and viewed through an upright microscope (E600FN, Nikon) equipped with DIC optics, epi-fluorescence, an infrared (IR) filter and an IR-sensitive video camera (C2400, Hamamatsu, Bridgewater, NJ, USA). Appropriate filter was used to visualize neurones retrogradely labelled with rhodamine.

Patch electrodes were pulled (Flaming/Brown P-97, Sutter Instrument, Novato, CA, USA) from borosilicate glass capillaries and polished to a tip resistance of 4–5 MΩ. Electrodes were filled with a solution containing (in mM): potassium gluconate, 135; Hepes, 10; EGTA, 0.1; $MgCl_2$, 1.0; NaCl, 1.0; Na_2ATP, 2.0; Na_2GTP, 0.5 (osmolarity 280–285 mosmol l^{-1}; pH 7.3). Note that a relatively low concentration of EGTA (0.1 mM) was used to allow intracellular free Ca^{2+} to accumulate and activate SK channels during membrane potential depolarization (Brenner *et al.* 2005). Whole-cell current- and voltage-clamp recordings were made using an Axopatch 200B amplifier and pCLAMP software (v10.0, Axon Instruments, Union City, CA, USA). The calculated liquid junction potential was −15 mV. Signals were filtered at 1 kHz, digitized at 10 kHz (Digidata 1322A, Axon Instruments), and saved on a computer for offline analysis. After achieving a gigaohm seal and the whole-cell configuration, cell capacitance, access resistance and resting membrane potential (V_m) were recorded until stable. Series resistance (16 ± 1 MΩ) was compensated in voltage-clamp recordings. Cells that met the following criteria were included in the analysis: action potential amplitude ≥50 mV from threshold to the peak, input resistance (R_{input}) larger than 0.5 GΩ when hyperpolarizing current injections of −20 pA were delivered from a holding potential of −80 mV, resting V_m negative to −50 mV, and less than 20% change in series resistance during the recording.

Identification of SK current

To study SK current, voltage-clamp recordings were performed with intracellular solution containing the cAMP analogue 8-(4-chlorophenylthio)-3′,5′-cyclic adenosine monophosphate (8CPT-cAMP, 50 μM) to block the slow after-hyperpolarization (sAHP) current (I_{sAHP}) (Stocker *et al.* 1999). Membrane potential was clamped at −60 mV and stepped to +10 mV for 100 ms. Upon returning V_m to −60 mV, an outward tail current was recorded. After control discharge responses were obtained, apamin (100 nM) or UCL1684 (100 nM) was bath applied to selectively block SK channels. A similar approach was used to assess the Ca^{2+} dependence of outward tail current. Stable tail currents were recorded under control conditions and slices were then perfused with Ca^{2+} free ACSF containing 2 mM $MgCl_2$. Tail current recorded during each treatment was subtracted from the corresponding control tail current to isolate SK-mediated current. Henceforth this current is referred to as I_{mAHP}. Recordings were performed in the presence of 1.0 μM tetrodotoxin (TTX) and 1 mM tetraethylammonium (TEA). Decay kinetics of the SK mediated I_{mAHP} were analysed by fitting the subtracted current with a one-phase exponential.

Testing neuronal excitability

Neuronal excitability was studied in current-clamp mode by adjusting V_m to −80 mV by injecting negative current through the patch electrode. Injected current was then varied in steps of +25 pA, each for a duration of 800 ms. To study the mAHP and ADP, recordings were made from a potential of −60 mV, and +150 pA current injections (500 ms) were made followed by a return of V_m to −60 mV for 5 s. To determine the spike threshold (V_t) and depolarizing R_{input} below V_t, ramp current injections (0.2 pA ms^{-1}, 1000 ms) were made from a potential of −80 mV. All current-clamp recordings were performed without TTX, TEA or 8CPT-cAMP.

Recording synaptic activity

To mimic conditions used in excitability testing, miniature excitatory postsynaptic currents (mEPSCs) were recorded in voltage-clamp mode at a holding potential of −80 mV. Recordings were performed in the presence of 1 μM TTX, 100 μM picrotoxin (a GABA-A receptor antagonist), and 2 mM $MgCl_2$ to block action potential dependent synaptic activity, GABAergic mIPSC activity, and NMDA receptor-mediated mEPSC activity. Effects of SK channel blockade on the frequency, amplitude and decay time constant of remaining AMPA receptor mediated mEPSC activity was determined by comparing events recorded under control conditions with those recorded from the same neurones during bath application of apamin (100 nM). Detection of events was accomplished by setting a threshold below the noise level, which was determined by bath application of 20 μM CNQX to block non-NMDA receptors.

Chemicals

All chemicals were obtained from Sigma-Aldrich (St Louis, MO, USA) with the exception of tetrodotoxin (Tocris Bioscience, UK) and tetraethylammonium (Fluka BioChemika, Switzerland).

Statistical analysis

Summary data are reported as means ± S.E.M. Depending on the experiment, group means were compared using either Student's *t*-test for unpaired data, or a

one-way or two-way ANOVA. When differences were found, Bonferroni's *post hoc* test was used for multiple pair-wise comparisons (GraphPad Prism, v5.0; GraphPad Software Inc., La Jolla, CA, USA). Mini-Analysis software (Synaptosoft, Leonia, NJ, USA) was used to analyse mEPSC activity. Cumulative probabilities of mEPSC inter-event intervals and amplitudes were compared using Kolomogorov–Smirnov tests. At least 200 mEPSCs were used for each analysis. Differences between means were considered significant at $P < 0.05$.

Results

Whole cell patch-clamp recording was performed on 45 retrogradely labelled PVN–RVLM neurones ($n = 25$ rats). Retrograde tracer was confined to the RVLM, which is located ventral to the nucleus ambiguus and 200–500 μm posterior to the caudal pole of the facial nucleus. Under conditions used in these experiments, recorded neurones lacked spontaneous discharge before and during SK channel blockade. This was the case except for two cells that had irregular spontaneous activity at relatively depolarized resting V_m (−48 mV). Data from these cells were excluded from analysis.

Identification of SK channel-mediated I_{mAHP} in PVN–RVLM neurons

In voltage-clamp recordings, SK current was isolated in a group of PVN–RVLM neurones that had a mean resting V_m of -58 ± 2 mV and a mean cell capacitance of 27 ± 4 pF ($n = 22$). To isolate SK current, V_m was stepped from a holding potential of −60 mV to +10 mV for 100 ms. Upon returning V_m to −60 mV, an outward tail current was observed. Bath application of the SK channel-selective blockers apamin and UCL1684 was used to isolate the SK current (I_{mAHP}) by subtraction. An apamin-sensitive I_{mAHP} was recorded in 4 of 4 neurones tested. Figure 1*A* shows a representative trace of isolated apamin-sensitive I_{mAHP} (Fig. 1*A*, inset). An UCL1684-sensitive I_{mAHP} was detected in another four cells. Figure 1*B* shows a representative trace of isolated UCL1684-sensitive I_{mAHP} (Fig. 1*B*, inset). As with SK channel blockade, perfusion with a Ca^{2+}-free bath solution (Fig. 1*C*, inset) effectively eliminated the tail

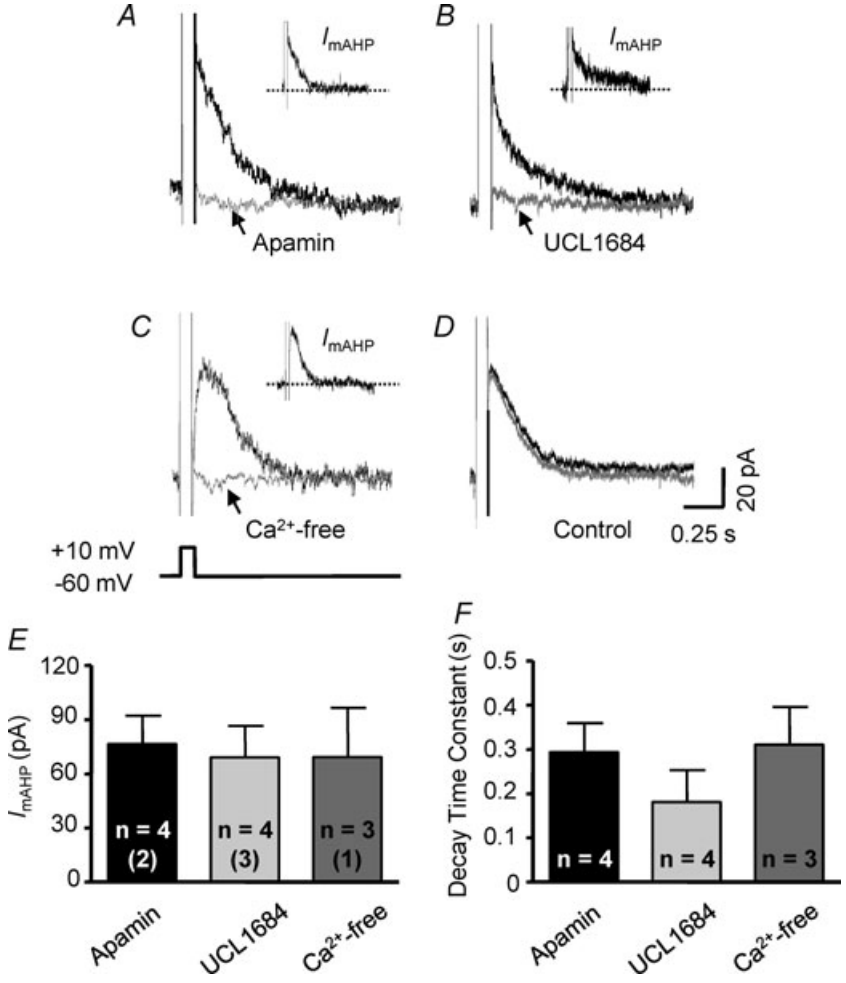

Figure 1. Characteristics of SK channel-mediated outward current in PVN–RVLM neurones
Representative traces show the outward tail current evoked by a 100 ms square pulse +70 mV depolarization (from −60 mV to +10 mV). Recordings were performed in the presence of bath TTX (1 μM) and TEA (1 mM), and intracellular 8CPT-cAMP (50 μM). *A* and *B*, outward tail current induced by the depolarizing pulse under control conditions (black trace) and in the presence of either apamin (*A*, grey trace, 100 nM) or UCL1684 (*B*, grey trace, 100 nM). Insets in *A* and *B* show net SK current (I_{mAHP}) obtained by subtraction (control – blocker). *C*, outward tail current was absent in Ca^{2+}-free ACSF. Inset in *C* shows the net SK current obtained from subtraction (control – Ca^{2+}-free). *D*, outward tail current under control conditions (black) was unchanged 15 min later (grey). *E*, summary data showing the amplitude of subtracted SK current (I_{mAHP}, left) and its decay time constant (right). The number of neurones recorded in each group is given inside the corresponding bar. Numbers in parentheses indicate number of animals from which data were obtained.

current. Neither the amplitude (Fig. 1*E*) nor the decay time constant (Fig. 1*F*) of I_{mAHP} was significantly different between cells treated with apamin and UCL1684 and Ca^{2+}-free extracellular solution. To test whether current rundown affected the amplitude of I_{mAHP}, time control experiments were performed ($n = 5$). Figure 1*D* shows representative traces of outward tail currents recorded immediately before and 15 min after switching to a second bath that also contained standard ACSF. Note that neither the amplitude (65.7 ± 18 *versus* 67.3 ± 21 pA) nor the decay time constant (285 ± 9 *versus* 318 ± 17 ms) changed significantly as a function of time.

Reversal potential of isolated I_{mAHP} was determined in voltage-clamp mode. Summary *I-V* relationships ($n = 6$) for subtracted I_{mAHP} were consistently non-rectifying. Reversal potential was −101 mV after correcting for liquid junction potential (Fig. 2*A*). This reversal potential was fairly close to the value predicted by the Nernest equation for a K^+ selective conductance, i.e. −103 mV. Figure 2*B* shows representative traces of apamin-sensitive I_{mAHP} evoked by voltage steps. These properties are consistent with those of voltage-insensitive, Ca^{2+}-activated SK channels.

SK channel blockade increases excitability of PVN–RVLM neurons

All neurones tested lacked spontaneous discharge, but depolarizing current injections consistently evoked repetitive action potential firing. Figure 3*Aa* shows a representative discharge response to a 200 pA depolarizing current pulse. The relationship between current injection and spike frequency (stimulus–response curve) was well fitted by a sigmoidal function. Graded current injections (25, 50, 75, 100, 125, 150, 175 and 200 pA; 800 ms) evoked graded increases in spike frequency (Fig. 3*Ba*).

The role of SK channels in regulating excitability was investigated by comparing the current–spike frequency relationship and the maximum discharge frequency response recorded in the absence and presence of SK channel blockers apamin and UCL1684. Figure 3*Ab* and *c* shows examples of action potential trains evoked by a 200 pA current pulse in the presence of apamin or UCL1684. Both blockers significantly increased the maximum firing rate compared to controls. Figure 3*Ba* plots mean spike frequency elicited by a family of graded depolarizing current steps (25 pA) for

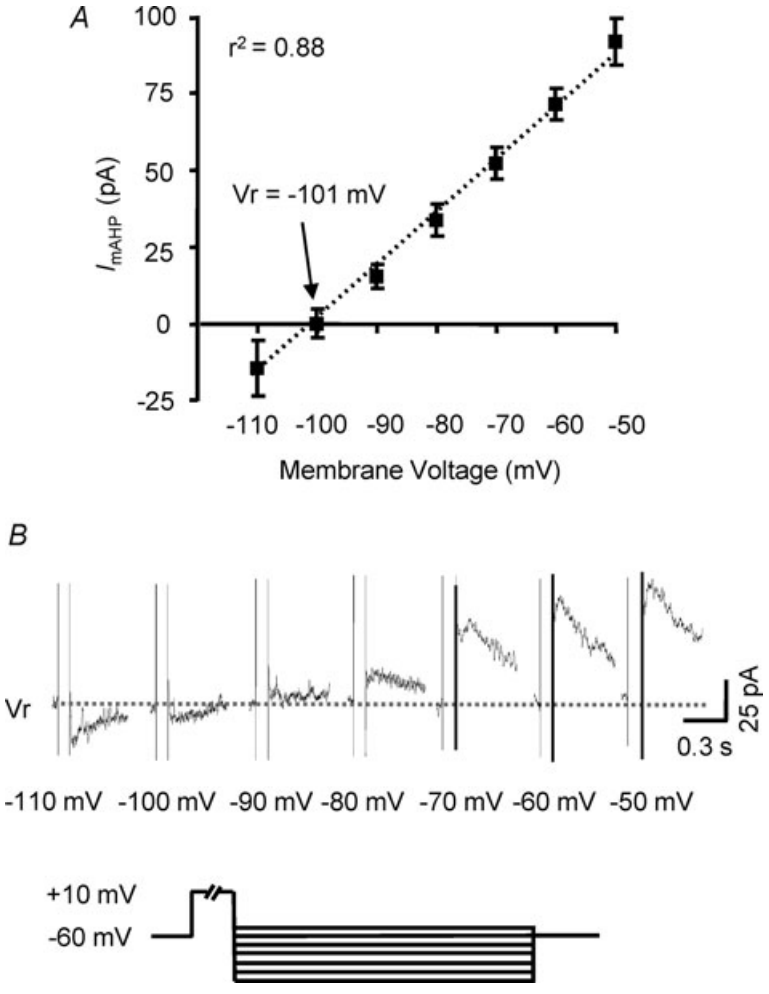

Figure 2. Reversal potential of SK current in PVN–RVLM neurones
A, mean amplitude of the subtracted SK current is plotted as a function of holding potential for PVN–RVLM neurones ($n = 6$) from 3 rats. Reversal potential was estimated to be −101 mV. *B*, representative subtracted SK current traces used to generate the *I–V* plot. To activate the outward current, a depolarizing pulse was delivered from a holding potential of −60 mV, followed by test potentials ranging from −110 mV to −50 mV in 10 mV increments.

groups of neurones in the absence and presence of SK channel blockers. Excitability was also compared by examining differences in the slope of stimulus–response curves. Responses evoked with currents between 0 and 125 pA were linear and the slope increased from 0.14 ± 0.01 Hz pA^{-1} in the absence of SK channel blockade to 0.25 ± 0.01 Hz pA^{-1} ($P < 0.01$) in the presence of apamin and 0.21 ± 0.03 Hz pA^{-1} ($P < 0.05$) in the presence of UCL1684 (Fig. 3*Bb*). It is worth noting that excitability was not significantly different between cells treated with apamin and UCL1684, although the discharge frequency and slope of stimulus–response curves for neurons treated with apamin were slightly greater than for neurones treated with UCL1684.

In the absence of SK channel blockade, neurones had a mean resting V_m of -66 ± 4 mV and a mean hyperpolarizing R_{input} of 1.2 ± 0.2 GΩ. The mean current needed to hyperpolarize V_m to near -80 mV was -17 ± 6 pA ($n = 7$). None of these values were affected by bath application of 100 nM apamin (resting V_m: -66 ± 2 mV; hyperpolarizing R_{input}: 1.1 ± 0.2 GΩ; mean current: -16 ± 4 pA; $n = 7$) or 100 nM UCL1684 (resting V_m: -63 ± 14 mV; hyperpolarizing R_{input}: 1.1 ± 0.1 GΩ; mean current: -16 ± 5 pA, $n = 5$). The hyperpolarizing R_{input} was measured by injecting a -20 pA current from a V_m very near to -80 mV.

SK channel blockade does not affect spike-frequency adaptation

Figure 3*Aa–c* shows that the pattern of inter-spike-interval (ISI) prolongation within action potential trains was not affected by SK channel blockade. In the absence of SK channel blockers (Fig. 3*Aa*), a 200 pA depolarizing current pulse evoked repetitive action potential firing that exhibited a progressive increase in ISI without causing complete termination of firing. In the presence of either apamin (Fig. 3*Ab*) or UCL1684 (Fig. 3*Ac*), mean spike frequency increased (Fig. 3*Ba*) but ISI prolongation (i.e. SFA) was unchanged, although the average ISI was significantly reduced by apamin (Fig. 3*Ca*) ($P < 0.01$) and by UCL1684 ($P < 0.05$). Summary data for the ratio of 13th ISI and 1st ISI are shown in Fig. 3*Cb*.

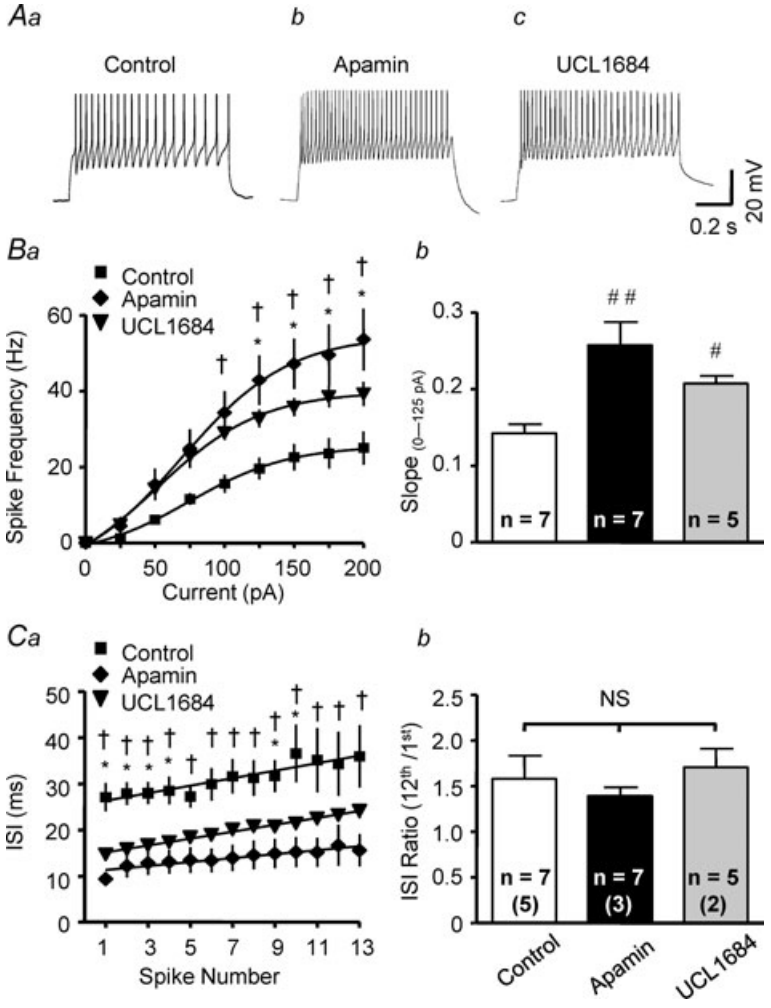

Figure 3. SK channel blockade increases excitability of PVN–RVLM neurones
Voltage traces show representative responses of PVN–RVLM neurones to a 200 pA depolarizing current injection (800 ms pulse) in the absence (*Aa*) and presence of SK channel blocker apamin (*Ab*, 100 nM) or UCL1684 (*Ac*, 100 nM). SFA is seen in *Aa–c*. *Ba*, the relationship between depolarizing current injected and spike frequency in the absence (Control, filled squares) and presence of apamin (filled rhombus) or UCL1684 (filled inverted triangles). Graded current injections evoked graded increases in spike frequency. The maximum spike frequency was achieved at ∼150 pA of depolarizing current. Apamin and UCL1684 each significantly increased the maximum spike frequency. Responses between 0 and 125 pA were nearly linear. Apamin and UCL1684 also increased the slope of the linear phase of the stimulus–response relation (*Bb*). *Ca*, plot showing inter-spike interval (ISI) during repetitive action potential firing in response to a 200 pA current injection. *Cb*, summary data showing the ratio of 13th ISI/1st ISI in the control condition and in the presence of SK channel blockers. SFA was evident in the absence and presence of SK channel blockade. #$P < 0.05$, ##$P < 0.01$ *versus* control, NS $P > 0.05$ (1-way ANOVA). *$P < 0.05$ UCL1684 *versus* control, †$P < 0.05$ apamin *versus* control (2-way ANOVA). The number of neurones recorded in each group is given inside the corresponding bar. Numbers in parentheses indicate number of animals from which data were obtained.

SK channel blockade reduces a medium AHP and reveals an ADP

To explore the mechanism of SK channel mediated suppression of excitability during action potential firing, the effect of SK channel blockade on the mAHP was examined. In current-clamp mode, depolarizing current pulses (150 pA, 500 ms) were injected from a V_m of −60 mV. Traces in Fig. 4*Aa–c* illustrate the mAHP and ADP recorded in cells with and without SK channel blockade. Under control conditions in the absence of an SK channel blocker (Fig. 4*Aa*), a train of action potentials was induced that exhibited SFA and a prominent mAHP following termination of action potential firing. In the presence of apamin (Fig. 4*Ab*) or UCL1684 (Fig. 4*Ac*) the mAHP was not observed, but a shoulder-shaped ADP was uncovered after the spike train. In the presence of apamin, the ADP was observed in 5 of 7 neurones tested. The peak amplitude was $+9 \pm 2$ mV (range: +3 to +17 mV) (Fig. 4*Ba*) and the decay time constant was 467 ± 175 ms (range: 158 to 1138 ms) (Fig. 4*Bb*). The other two cells had smaller amplitude of mAHP (-5 ± 2 mV) compared to those recorded under control condition (-8 ± 2 mV). No ADP was uncovered in these cells. In the presence of UCL1684, an ADP was observed in 5 of 5 neurones tested. Peak ADP amplitude in these cells was $+8 \pm 1$ mV (range: +5 to +13 mV) (Fig. 4*Ba*) and the decay time constant was 416 ± 123 ms (range: 48–831 ms) (Fig. 4*Bb*).

SK channel blockade increases depolarizing R_{input} without alteration of V_t

To determine whether SK channel blockade affects action potential voltage threshold (V_t) and depolarizing R_{input} in PVN–RVLM neurones, ramp current injection was performed. Current ramps induced gradual membrane potential depolarization (0.2 pA ms^{-1} for 1000 ms duration) and triggered action potentials at V_t (Fig. 5*Aa–c*, summarized in Fig. 5*Bc*). Blockade of SK channels increased the rate of depolarization such that V_t was reached earlier during the current ramp (Fig. 5*Ab* and *c*). Thus, depolarizing R_{input} measured below V_t was significantly increased ($P < 0.05$) by both apamin and UCL1684 compared to control (Fig. 5*Ba*). Similar to effects of SK channel blockade on responses to depolarizing current pulses (Fig. 3*Aa–c*), firing rate of spikes evoked by current ramps was significantly increased in the presence of apamin and UCL1684 (Fig. 5*Bb*). Note that there was no effect of SK channel blockade on V_t (Fig. 5*Bc*).

SK channel blockade does not affect mEPSCs

Traces in Fig. 6*Aa* and *b* illustrate mEPSCs recorded in a cell under control conditions (Fig. 6*Aa*) and after application of 100 nM apamin (Fig. 6*Ab*). Application of 20 μM CNQX (a glutamate non-NMDA receptor antagonist) effectively abolished mEPSCs (Fig. 6*Ac*). The insets in Fig. 6*Aa* and *b* show the decay time constant (τ) of mEPSCs obtained from control and during bath application of apamin. The decay phase of mEPSCs was best fitted with a one-phase exponential function. The τ was similar during control and bath application of apamin as summarized in Fig. 6*Cc*. Cumulative probability analysis of mEPSCs in the same cell revealed that SK channel blockade did not affect the distribution pattern of inter-event intervals (Fig. 6*Ba*) and event amplitudes (Fig. 6*Bb*). Bath application of apamin did not

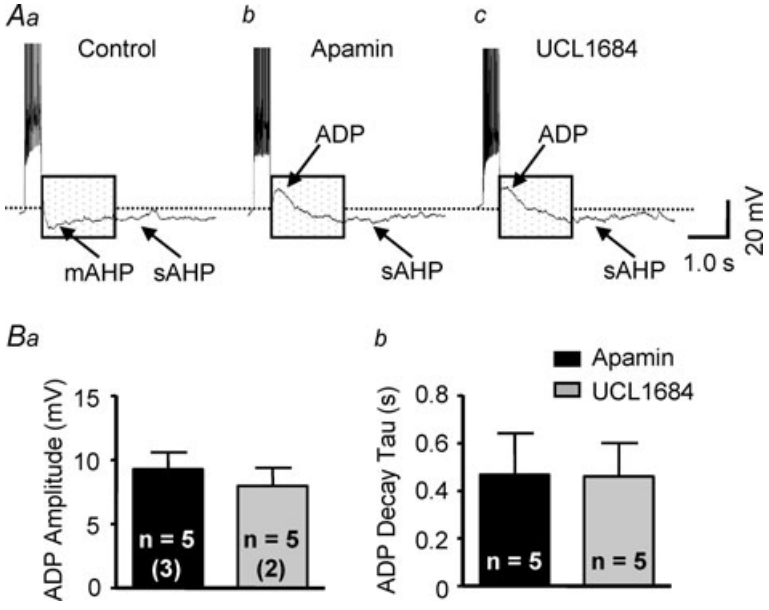

Figure 4. SK channel blockade reduces mAHP and uncovers an ADP
Representative voltage traces show the effect of SK channel blockade on the medium after-hyperpolarizing potential (mAHP). *Aa*, in the absence of SK channel blockade, a train of action potentials was induced by a depolarizing current pulse (150 pA, 500 ms). Both a mAHP and slow AHP (sAHP) were observed following termination of action potential firing. *Ab* and *Ac*, in the presence of apamin (*Ab*; 100 nM) and UCL1684 (*Ac*; 100 nM), a shoulder-shaped after-depolarizing potential (ADP) was revealed. Note that the sAHP can still be observed. *B*, summary data showing that the maximum ADP amplitude (*Ba*) and the ADP decay time constant (*Bb*) were similar in the presence of apamin and UCL1684. The number of neurones recorded in each group is given inside the corresponding bar. Numbers in parentheses indicate number of animals from which data were obtained.

affect mean frequency and amplitude of mEPSC (Fig. 6*Ca* and *b*). Neurones had a mean resting V_m of -53 ± 2 mV and mean holding current of -23 ± 8 pA when the cell was clamped at -80 mV. Neither was significantly affected by apamin (resting V_m: -55 ± 4 mV, holding current: -25 ± 7 pA, $n = 4$).

Discussion

Although synaptic and intrinsic mechanisms contribute to spontaneous action potential firing in PVN–RVLM neurones (Sonner & Stern, 2007; Li *et al.* 2008), mechanisms controlling their excitability have not been extensively studied. Here we report that PVN–RVLM neurones express an apamin-sensitive SK current. We found that depolarizing step current injections evoked trains of action potentials that underwent SFA. Upon termination of current injection, a prominent mAHP was observed. Blockade of SK channels did not change the rate of SFA, but did increase the frequency of current-induced spiking. SK channel blockade also abolished the mAHP and revealed a prominent ADP. The increased rate of current-induced spiking during SK channel blockade, therefore, is likely to be due to the loss of mAHP-mediated opposition of the ADP. SK channel blockade did not change resting V_m, but did increase depolarizing R_{input} at membrane potentials below spike threshold. Thus SK channel activation in PVN–RVLM neurons appears to occur between resting V_m and spike threshold. Consistent with effects of SK channel blockade being mediated postsynaptically, bath application of apamin had no effect on the frequency, amplitude or decay time constant of mEPSCs. Taken together, these findings provide new evidence that activation of SK channels can modulate intrinsic membrane properties of presympathetic PVN–RVLM neurones and can strongly suppress their *in vitro* excitability.

Excitability of PVN–RVLM neurones is regulated by SK current

In this study, PVN–RVLM neurones displayed consistent SFA with a near linear rate of ISI prolongation (Fig. 3*Ca*) that was essentially unchanged by SK channel blockade. This suggests that SFA in PVN–RVLM neurons is largely controlled by channels other than SK channels. Consistent with this conclusion was our observation that PVN–RVLM neurones exhibited an obvious sAHP (Fig. 4). Therefore, an apamin-insensitive I_{sAHP} (Vogalis *et al.* 2003; Teagarden *et al.* 2008) might be responsible for the SFA in these neurones. Alternatively, M current

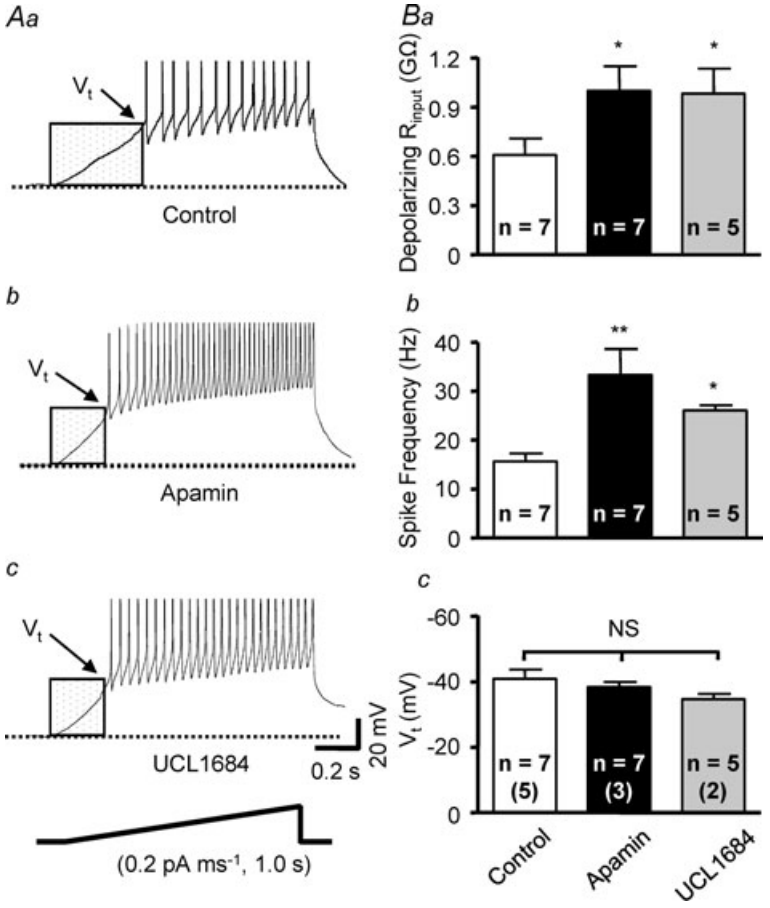

Figure 5. SK channel blockade increases depolarizing input resistance below spike threshold
Traces show representative responses of PVN–RVLM neurones to ramp current injections in the absence (*Aa*, control) and presence of the SK channel blockers apamin (*Ab*, 100 nM) and UCL1684 (*Ac*, 100 nM). Under each treatment, membrane potential depolarized gradually in response to current injection (0.2 pA ms^{-1}, 1000 ms) and action potential firing began at the potential threshold (V_t). SK channel blockade with apamin or UCL1684 increased subthreshold depolarization rate by increasing the depolarizing input resistance (R_{input}). V_t (arrows) for triggering action potentials did not change although the action potential firing rate was increased by bath application of apamin and UCL1684. *B*, summary data showing that depolarizing R_{input} (*Ba*) and action potential firing rate (*Bb*) during ramp current injections were significantly increased by SK channel blockade. Blocking SK channels with either apamin or UCL1684 caused a slight depolarizing shift of V_t, but these changes did not reach statistical significance (*Bc*). $^*P < 0.05$ *versus* control, $^{**}P < 0.01$ *versus* control, NS $P > 0.05$ (1-way ANOVA). The number of neurones recorded in each group is given inside the corresponding bar. Numbers in parentheses indicate number of animals from which data were obtained.

could be involved (Yue & Yaari, 2004; Gu *et al*. 2005; Wu *et al*. 2008), although we are unaware of evidence that PVN–RVLM neurones express KCNQ channels. Whatever channels mediate SFA in PVN–RVLM neurones, it should be emphasized that although SK channel blockade did not alter the rate of ISI prolongation, it did significantly increase current-evoked discharge frequency overall. Therefore, we would speculate that negative modulation or loss of SK channel function *in vivo* could lead to increased discharge of PVN–RVLM neurons.

Another observation in the present study was that blocking SK channels increased sub-threshold depolarizing R_{input} without altering action potential threshold. Together these effects increased the rate of depolarization and reduced the spike latency. The mechanism responsible for increasing depolarizing R_{input} during SK channel blockade is not known. It seems likely, however, that block of SK channels is a direct contributing factor since our data indicate that they activate at membrane potentials between resting V_m and spike threshold. The fact that blockade of SK channels had no effect on resting V_m supports the view that they are activated by the increase in calcium influx through voltage-dependent calcium channels during depolarization.

It should be mentioned that the excitability of cells treated with apamin was greater than cells treated with UCL1684 even though the difference did not reach statistical significance. The explanation for this could be that the concentration of UCL1684 we used was lower than that of apamin owing to the former being less soluble in aqueous solution.

Resting V_m and spontaneous discharge are unaffected by SK channel blockade

In GnRH neurones (Liu & Herbison, 2008) and supra-chiasmatic nucleus neurones (Teshima *et al*. 2003), SK channels have been reported to contribute to resting V_m and to restrain *in vitro* spontaneous discharge. In this study, SK channel blockade had no effect on either resting V_m or spontaneous discharge of PVN–RVLM neurones. Our findings are consistent with those of Li & Pan (2006) who showed that even a 500 nM concentration of apamin failed to alter spontaneous firing of PVN–RVLM neurones. Collectively, these findings indicate that SK channels are not tonically active in PVN–RVLM neurons at resting V_m in brain slices. It is not known if the same holds true for neurons *in vivo*. In brain slices, extrinsic synaptic inputs are eliminated and therefore loss of excitatory inputs could reduce Ca^{2+} influx, thereby causing *in vitro* activity of SK channels to be artificially low. In the case of PVN–RVLM neurones, eliminating glutamatergic

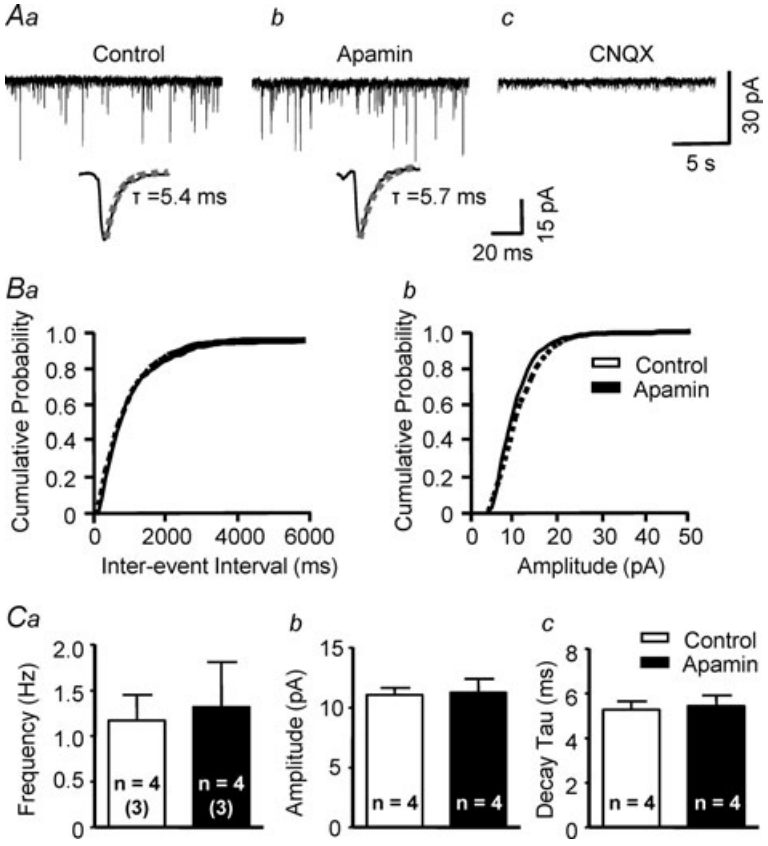

Figure 6. Lack of effect of SK channel blockade on mEPSCs in PVN–RVLM neurones
Representative traces from a PVN–RVLM neurone show miniature excitatory postsynaptic currents (mEPSCs) during voltage-clamp recording at a holding potential of −80 mV. Recordings were performed in the presence of TTX (1 μM) and picrotoxin (100 μM). *Aa* and *Ab*, spontaneous mEPSCs under control condition and in the presence of apamin (100 nM). Inset in *Aa* and *Ab* shows the decay time constant (τ) of mEPSCs obtained from control and during bath application of apamin. The decay phase of mEPSCs was best fitted with one-phase exponential function. The decay time constant was similar during control and bath application of apamin (*Cc*). *Ac*, bath application of 20 μM CNQX effectively abolished mEPSCs. Cumulative probability plots of mEPSCs from the same neurone show that the distribution of the inter-event intervals (*Ba*) and amplitudes (*Bb*) during control condition and in the presence of apamin. Summary data show the lack of effect of apamin on the frequency (*Ca*), amplitude (*Cb*), or decay time constant (*Cc*) of mEPSCs in PVN–RVLM neurones. The number of neurones recorded in each group is given inside the corresponding bar. Numbers in parentheses indicate number of animals from which data were obtained.

input from the forebrain (Grob *et al*. 2003) and other hypothalamic nuclei (Boudaba *et al*. 1997; Csáki *et al*. 2000) would reduce Ca^{2+} influx through NMDA receptors (Ngo-Anh *et al*. 2005) and possibly through low- and high-voltage activated Ca^{2+} channels, thereby possibly preventing tonic activation of SK channels.

In the present study all but two neurones were quiescent and remained so during SK channel blockade. By contrast, previous slice studies reported that most PVN–RVLM neurones fired spontaneously and had values of resting V_m that were depolarized compared to those in the present study (Cato & Toney, 2005; Li & Pan, 2006; Park *et al*. 2007). These discrepancies are likely to be explained by the fact that the previous studies were carried out during blockade of glutamatergic and GABAergic inputs. Indeed, GABA-A receptor blockade with bicuculline methiodide (BMI) has been reported to depolarize V_m of PVN–RVLM neurones and to increase their *in vitro* firing rate (Li & Pan, 2006) and their excitability (Park *et al*. 2007). Given that the GABA-A receptor antagonist BMI can also block SK channels, it is possible that effects could have involved actions at both sites. However, the lack of effect of apamin and UCL1684 to change resting V_m or to induce discharge in the present study suggests that previously reported actions of BMI are most likely to have been due to blockade of GABA-A receptors. Consistent with this, the present study found that resting V_m was relatively depolarized (−53 mV) when recordings were performed in the presence of another GABA-A receptor antagonist, picrotoxin (see Fig. 6).

I_{mAHP} in PVN–RVLM neurones is mediated by SK channels

Large amplitude and long duration AHPs, including the mAHP, develop as a consequence of intracellular Ca^{2+} accumulation during repetitive action potential firing (Stocker, 2004; Bond *et al*. 2005). Interestingly, blockade of SK channels in the present study not only reduced the amplitude of the mAHP, but revealed the presence of an ADP. Thus, it appears that opposing actions of the mAHP and the ADP normally participate in setting the rate of firing in response to stimulation. Typically, voltage-dependent Ca^{2+} influx activates Ca^{2+}-dependent K^+ conductance that underlies AHPs. In addition to inhibiting neuronal firing, depolarization and Ca^{2+} influx can also increase firing rate through activation of a non-selective cation current (Ghamari-Langroudi & Bourque, 2002; Teruyama & Armstrong, 2007). The current underlying the ADP has been proposed to be a Ca^{2+}-activated current rather than a Ca^{2+} current *per se* as it is abolished by strongly buffering intracellular Ca^{2+} with BAPTA (Teruyama & Armstrong, 2007). Consistent with our findings, blockade of SK channels with apamin has been reported to also reveal an ADP and increase the firing of gonadotropin-releasing hormone neurones (Liu & Herbison, 2008) and neocortical layer pyramidal neurones (Higgs & Spain, 2009). These findings indicate that the ability of SK channels to limit excitability of PVN–RVLM neurones is likely to result from their role in evoking/modulating a mAHP that oppose the ADP in these neurones.

Blockade of SK channels does not alter glutamatergic activity in PVN–RVLM neurones

It should be emphasized that although we observed a prominent SK current in PVN–RVLM neurones, increased excitability resulting from bath application of SK channel blockers may not be entirely due to post-synaptic actions. We therefore investigated whether bath application of apamin was accompanied by increased excitatory synaptic input that might also contribute to increased excitability. Such seems unlikely given our observation of increased depolarizing R_{input} in the presence of apamin. Nevertheless, SK3 channels have been localized to nerve terminals in cultured hippocampal neurones (Obermair *et al*. 2003) and at the neuromuscular junction (Roncarati *et al*. 2001), and this raises at least the possibility that they modulate terminal release of transmitter. However, apamin treatment did not affect the frequency, amplitude or decay time constant of mEPSCs recorded from PVN–RVLM neurones. Therefore it seems most likely that SK channels expressed postsynptically in PVN–RVLM neurones are the main site at which blockers acted in this study to increase excitability.

Conclusions

In summary, findings from this study strongly suggest that SK channels play an important role in regulating excitability of PVN–RVLM neurones. Blockade of SK channels increases *in vitro* spike discharge of PVN–RVLM neurones in response to current injections. The mechanism appears to involve both an increase in the depolarizing R_{input} below spike threshold and reduced mAHP during repetitive action potential firing. The latter may oppose a prominent ADP expressed in these cells.

When SK channels of PVN–RVLM neurones are blocked, how does this affect the activity of downstream neurones in the RVLM? This will be an important question to answer in order to understand how regulation of this pathway affects sympathetic nervous system outflow under physiological and disease conditions. It has been reported that activation of the PVN increases the discharge of bulbospinal vasomotor neurones in the RVLM (Yang & Coote, 1998; Yang *et al*. 2001) and a recent study reported that water deprivation induced activation of

a prominent glutamatergic pathway from the PVN to the RVLM (Stocker *et al*. 2006). Considering the fact that blockade of SK channels in PVN–RVLM neurones increased their excitability, we speculate that negative modulation or loss of SK channel function in these neurones could increase glutamatergic activation of RVLM vasomotor neurones. Such an effect could play an important role in PVN-mediated activation of sympathetic vasomotor tone that occurs under physiological conditions (Stocker *et al*. 2005; Cruz *et al*. 2008; Reddy *et al*. 2007), in metabolic disorders (Perin *et al*. 2001; Zheng *et al*. 2006; Stocker *et al*. 2007) and in cardiovascular diseases (Zucker *et al*. 2001; Felder *et al*. 2001; Sonner *et al*. 2008).

References

Akine A, Montanaro M & Allen AM (2003). Hypothalamic paraventricular nucleus inhibition decreases renal sympathetic nerve activity in hypertensive and normotensive rats. *Auton Neurosci* **108**, 17–21.

Allen AM (2002). Inhibition of the hypothalamic paraventricular nucleus in spontaneously hypertensive rats dramatically reduces sympathetic vasomotor tone. *Hypertension* **39**, 275–280.

Bond CT, Maylie J & Adelman JP (2005). SK channels in excitability, pacemaking and synaptic integration. *Curr Opin Neurobiol* **15**, 305–311.

Boudaba C, Schrader LA & Tasker JG (1997). Physiological evidence for local excitatory synaptic circuits in the rat hypothalamus. *J Neurophysiol* **77**, 3396–3400.

Brenner R, Chen QH, Vilaythong A, Toney GM, Noebels JL & Aldrich RW (2005). BK channel $\beta 4$ subunit reduces dentate gyrus excitability and protects against temporal lobe seizures. *Nat Neurosci* **8**, 1752–1759.

Cato MJ & Toney GM (2005). Angiotensin II excites paraventricular nucleus neurons that innervate the rostral ventrolateral medulla: an in vitro patch-clamp study in brain slices. *J Neurophysiol* **93**, 403–413.

Chen QH & Toney GM (2000). Discharge properties and osmotic responsiveness of hyperthalamic PVN neurons projecting to the rostral ventrolateral medulla (abstract). *FASEB J* **14**, A626.

Chen QH & Toney GM (2003). Identification and characterization of two functionally distinct groups of spinal cord-projecting paraventricular nucleus neurons with sympathetic-related activity. *Neuroscience* **118**, 797–807.

Chen QH, Haywood JR & Toney GM (2003). Sympathoexcitation by PVN-injected bicuculline requires activation of excitatory amino acid receptors. *Hypertension* **42**, 725–731.

Cruz JC, Bonagamba LG, Machado BH, Biancardi VC & Stern JE (2008). Intermittent activation of peripheral chemoreceptors in awake rats induces Fos expression in rostral ventrolateral medulla-projecting neurons in the paraventricular nucleus of the hypothalamus. *Neuroscience* **157**, 463–472.

Csáki A, Kocsis K, Halász B & Kiss J (2000). Localization of glutamatergic/aspartatergic neurons projecting to the hypothalamic paraventricular nucleus studied by retrograde transport of [3H]D-aspartate autoradiography. *Neuroscience* **101**, 637–655.

Jenkinson DH (2006). Potassium channels – multiplicity and challenges. *Br J Pharmacol* **147**, S63–S71.

Felder RB, Francis J, Weiss RM, Zhang ZH, Wei SG & Johnson AK (2001). Neurohumoral regulation in ischemia-induced heart failure. Role of the forebrain. *Ann N Y Acad Sci* **940**, 444–453.

Ghamari-Langroudi M & Bourque CW (2002). Flufenamic acid blocks depolarizing afterpotentials and phasic firing in rat supraoptic neurones. *J Physiol* **545**, 537–542.

Grob M, Trottier JF, Drolet G & Mouginot D (2003). Characterization of the neurochemical content of neuronal populations of the lamina terminalis activated by acute hydromineral challenge. *Neuroscience* **122**, 247–257.

Gu N, Vervaeke K, Hu H & Storm JF (2005). Kv7/KCNQ/M and HCN/h, but not KCa2/SK channels, contribute to the somatic medium after-hyperpolarization and excitability control in CA1 hippocampal pyramidal cells. *J Physiol* **566**, 689–715.

Guyenet PG (2006). The sympathetic control of blood pressure. *Nat Rev Neurosci* **7**, 335–346.

Haywood JR, Mifflin SW, Craig T, Calderon A, Hensler JG & Hinojosa-Laborde C (2001). γ-Aminobutyric acid (GABA)-A function and binding in the paraventricular nucleus of the hypothalamus in chronic renal-wrap hypertension. *Hypertension* **37**, 614–618.

Higgs MH & Spain WJ (2009). Conditional bursting enhances resonant firing in neocortical layer 2–3 pyramidal neurons. *J Neurosci* **29**, 1285–1299.

Kenney MJ, Weiss ML, Patel KP, Wang Y & Fels RJ (2001). Paraventricular nucleus bicuculline alters frequency components of sympathetic nerve discharge bursts. *Am J Physiol Heart Circ Physiol* **281**, H1233–1241.

Kleiber AC, Zheng H, Schultz HD, Peuler JD & Patel KP (2008). Exercise training normalizes enhanced glutamate-mediated sympathetic activation from the PVN in heart failure. *Am J Physiol Regul Integr Comp Physiol* **294**, R1863–1872.

Li DP & Pan HL (2006). Plasticity of GABAergic control of hypothalamic presympathetic neurons in hypertension. *Am J Physiol Heart Circ Physiol* **290**, H1110–1119.

Li DP & Pan HL (2007). Glutamatergic inputs in the hypothalamic paraventricular nucleus maintain sympathetic vasomotor tone in hypertension. *Hypertension* **49**, 916–925.

Li DP, Yang Q, Pan HM & Pan HL (2008). Pre- and postsynaptic plasticity underlying augmented glutamatergic inputs to hypothalamic presympathetic neurons in spontaneously hypertensive rats. *J Physiol* **586**, 1637–1647.

Liu X & Herbison AE (2008). Small-conductance calcium-activated potassium channels control excitability and firing dynamics in gonadotropin-releasing hormone (GnRH) neurons. *Endocrinology* **149**, 3598–3604.

Lovick TA & Coote JH (1988). Electrophysiological properties of paraventriculo-spinal neurones in the rat. *Brain Res* **454**, 123–130.

Martin DS, Segura T & Haywood JR (1991). Cardiovascular responses to bicuculline in the paraventricular nucleus of the rat. *Hypertension* **18**, 48–55.

Ngo-Anh TJ, Bloodgood BL, Lin M, Sabatini BL, Maylie J & Adelman JP (2005). SK channels and NMDA receptors form a Ca^{2+}-mediated feedback loop in dendritic spines. *Nat Neurosci* **8**, 642–649.

Obermair GJ, Kaufmann WA, Knaus HG & Flucher BE (2003). The small conductance Ca^{2+}-activated K^+ channel SK3 is localized in nerve terminals of excitatory synapses of cultured mouse hippocampal neurons. *Eur J Neurosci* **17**, 721–731.

Pakhomov AG, Semenov I, Brenner R & Toney GM (2006). Hydraulically coupled microejection technique for precise local solution delivery in tissues. *J Neurosci Methods* **155**, 231–240.

Park JB, Skalska S, Son S & Stern JE (2007). Dual $GABA_A$ receptor-mediated inhibition in rat presympathetic paraventricular nucleus neurons. *J Physiol* **582**, 539–551.

Pedarzani P, Kulik A, Muller M, Ballanyi K & Stocker M (2000). Molecular determinants of Ca^{2+}-dependent K^+ channel function in rat dorsal vagal neurones. *J Physiol* **527**, 283–290.

Perin PC, Maule S & Quadri R (2001). Sympathetic nervous system, diabetes, and hypertension. *Clin Exp Hypertens* **23**, 45–55.

Porter JP & Brody MJ (1985). Neural projections from paraventricular nucleus that subserve vasomotor functions. *Am J Physiol Regul Integr Comp Physiol* **248**, R271–281.

Reddy MK, Schultz HD, Zheng H & Patel KP (2007). Altered nitric oxide mechanism within the paraventricular nucleus contributes to the augmented carotid body chemoreflex in heart failure. *Am J Physiol Heart Circ Physiol* **292**, H149–157.

Roncarati R, Di Chio M, Sava A, Terstappen GC & Fumagalli G (2001). Presynaptic localization of the small conductance calcium-activated potassium channel SK3 at the neuromuscular junction. *Neuroscience* **104**, 253–262.

Sonner PM & Stern JE (2007). Functional role of A-type potassium currents in rat presympathetic PVN neurones. *J Physiol* **582**, 219–238.

Sonner PM, Filosa JA & Stern JE (2008). Diminished A-type potassium current and altered firing properties in presympathetic PVN neurones in renovascular hypertensive rats. *J Physiol* **586**, 1605–1622.

Stern JE (2001). Electrophysiological and morphological properties of pre-autonomic neurones in the rat hypothalamic paraventricular nucleus. *J Physiol* **537**, 161–177.

Stocker M (2004). Ca^{2+}-activated K^+ channels: molecular determinants and function of the SK family. *Nat Rev Neurosci* **5**, 758–770.

Stocker M, Krause M & Pedarzani P (1999). An apamin-sensitive Ca^{2+}-activated K^+ current in hippocampal pyramidal neurons. *Proc Natl Acad Sci U S A* **96**, 4662–4667.

Stocker SD, Cunningham JT & Toney GM (2004*a*). Water deprivation increases Fos immunoreactivity in PVN autonomic neurons with projections to the spinal cord and rostral ventrolateral medulla. *Am J Physiol Regul Integr Comp Physiol* **287**, R1172–1183.

Stocker SD, Keith KJ & Toney GM (2004*b*). Acute inhibition of the hypothalamic paraventricular nucleus decreases renal sympathetic nerve activity and arterial blood pressure in water-deprived rats. *Am J Physiol Regul Integr Comp Physiol* **286**, R719–725.

Stocker SD, Hunwick KJ & Toney GM (2005). Hypothalamic paraventricular nucleus differentially supports lumbar and renal sympathetic outflow in water-deprived rats. *J Physiol* **563**, 249–263.

Stocker SD, Simmons JR, Stornetta RL, Toney GM & Guyenet PG (2006). Water deprivation activates a glutamatergic projection from the hypothalamic paraventricular nucleus to the rostral ventrolateral medulla. *J Comp Neurol* **494**, 673–685.

Stocker SD, Meador R & Adams JM (2007). Neurons of the rostral ventrolateral medulla contribute to obesity-induced hypertension in rats. *Hypertension* **49**, 640–646.

Tasker JG & Dudek FE (1991). Electrophysiological properties of neurones in the region of the paraventricular nucleus in slices of rat hypothalamus. *J Physiol* **434**, 271–293.

Teagarden M, Atherton JF, Bevan MD & Wilson CJ (2008). Accumulation of cytoplasmic calcium, but not apamin-sensitive afterhyperpolarization current, during high frequency firing in rat subthalamic nucleus cells. *J Physiol* **586**, 817–833.

Teruyama R & Armstrong WE (2007). Calcium-dependent fast depolarizing afterpotentials in vasopressin neurons in the rat supraoptic nucleus. *J Neurophysiol* **98**, 2612–2621.

Teshima K, Kim SH & Allen CN (2003). Characterization of an apamin-sensitive potassium current in suprachiasmatic nucleus neurons. *Neuroscience* **120**, 65–73.

Toney GM, Chen QH, Cato MJ & Stocker SD (2003). Central osmotic regulation of sympathetic nerve activity. *Acta Physiol Scand* **177**, 43–55.

Villalobos C, Shakkottai VG, Chandy KG, Michelhaugh SK & Andrade R (2004). SK_{Ca} channels mediate the medium but not the slow calcium-activated afterhyperpolarization in cortical neurons. *J Neurosci* **24**, 3537–3542.

Vogalis F, Storm JF & Lancaster B (2003). SK channels and the varieties of slow after-hyperpolarizations in neurons. *Eur J Neurosci* **18**, 3155–3166.

Wu WW, Chan CS, Surmeier DJ & Disterhoft JF (2008). Coupling of L-type Ca^{2+} channels to KV7/KCNQ channels creates a novel, activity-dependent, homeostatic intrinsic plasticity. *J Neurophysiol* **100**, 1897–1908.

Yang Z & Coote JH (1998). Influence of the hypothalamic paraventricular nucleus on cardiovascular neurons in the rostral ventrolateral medulla of the rat. *J Physiol* **513**, 521–530.

Yang Z, Bertram D & Coote JH (2001). The role of glutamate and vasopressin in the excitation of RVL neurones by paraventricular neurones. *Brain Res* **908**, 99–103.

Yue C & Yaari Y (2004). KCNQ/M channels control spike afterdepolarization and burst generation in hippocampal neurons. *J Neurosci* **24**, 4614–4624.

Zheng H, Mayhan WG, Bidasee KR & Patel KP (2006). Blunted nitric oxide-mediated inhibition of sympathetic nerve activity within the paraventricular nucleus in diabetic rats. *Am J Physiol Regul Integr Comp Physiol* **290**, R992–1002.

Zucker IH, Wang W, Pliquett RU, Liu JL & Patel KP (2001). The regulation of sympathetic outflow in heart failure. The roles of angiotensin II, nitric oxide, and exercise training. *Ann N Y Acad Sci* **940**, 431–443.

Author contributions

Q.-H.C. designed and performed the research, analysed and interpreted data and wrote the manuscript. G.M.T. interpreted data and revised the manuscript. These experiments were performed in the Department of Physiology, University of Texas Health Science Center at San Antonio.

Acknowledgments

This study was funded by NIH grants HL-076312 (GMT) and HL071645 (GMT) and American Heart Association grant AHA0865107F (QHC). We thank Dr Robert Brenner for critically reviewing the manuscript. The authors gratefully acknowledge Mary Ann Andrade and Alfredo S. Calderon for technical assistance.